Bare Density of States at the Fermi Level in $V_3Ga_{1-x}Sn_x$: A Nuclear-Magnetic-Resonance Study*

F. Y. Fradin and D. Zamir†
Argonne National Laboratory, Argonne, Illinois 60439
(Received 24 October 1972)

The superconducting transition temperature of the pseudobinary $A15$ compounds $V_3Ga_{1-x}Sn_x$ ($0 \leq x \leq 1$) falls sharply from a peak of about 14 °K at $x=0$ to about 4 °K at $x=1$. In order to understand the dependence of T_c on the electronic structure, we have measured the spin-lattice relaxation rate, isotropic and axial Knight shift, and electric field gradient of ^{51}V in the normal and superconducting state at frequencies between 8 and 48.5 MHz. The composition dependence of the relaxation rate and the electric field gradient are calculated by a tight-binding model and the theory of Watson, Gossard, and Yafet, respectively. The results are in quantitative agreement with the d-subband densities of states based on an interpolation of the augmented-plane-wave band-structure calculations of Mattheiss. Symmetry considerations suggest that the difference in the electron-phonon coupling parameter for V_3Ga and V_3Sn could be due to an anomalously large phonon renormalization in V_3Ga caused by a peak in the π-subband density at the Fermi level.

I. INTRODUCTION

The problem of understanding the high-transition-temperature superconductors among the transition-metal alloys and intermetallic compounds has in recent years been reduced to explaining the variation of the electron-phonon coupling constant $\lambda = m^*/m - 1$. A generalization[1] of McMillan's equation[2] for the superconducting transition temperature T_c is given by

$$T_c = \frac{\langle\omega^2\rangle^{1/2}}{1.20} \exp\left(-\frac{1+\lambda+\mu_{\text{spin}}}{0.96\lambda - (\mu^*+\mu_{\text{spin}})(1+0.6\lambda)}\right). \quad (1.1)$$

Here μ^* is the Coulomb pseudopotential, μ_{spin} is the effective electron-spin excitation coupling constant, and $\langle\omega^2\rangle$ is a weighted phonon frequency. μ^* is a slowly varying function of the bare density of states at the Fermi level $N(0)$, having values between about 0.1 and 0.2 for most transition metals.[1] μ_{spin} can be approximately determined from spin-susceptibility measurements[3] and $\langle\omega^2\rangle^{1/2}$ can be estimated from phonon-specific-heat measurements.

In McMillan's formulation λ depends on both the electronic and phonon properties and is given by

$$\lambda = \frac{N(0)\langle I^2\rangle}{M\langle\omega\rangle/\langle\omega^{-1}\rangle}, \quad (1.2)$$

where $\langle I^2\rangle$ is an average over the Fermi surface of the electron-ion interaction and M is the ion mass. In many high-T_c materials, there has been growing evidence that soft-phonon modes are present. This has been deduced from neutron-inelastic-scattering, elastic-constant, nuclear-magnetic-resonance, and Mössbauer-effect measurements.[4] In some materials a martensitic transformation takes place above T_c. In one class of particularly important high-temperature superconductors, the $A15$ compounds V_3X and Nb_3X, which have the highest known T_c's, an extremely high narrow peak in the density of states is thought to play an important role.[5] Of course, the separation of the electron and phonon systems is somewhat artificial since electron dressing of the phonon states is probably quite important. It seems that much of the difficulty in the detailed explanation of superconductivity in the transition metals in general, and the $A15$ compounds in particular, lies in the need for more experimental property measurements and theoretical calculations of the normal-state properties; i.e., the electron-phonon interaction, the one-electron density of states, and the phonon spectral densities.

In this investigation we present results of a nuclear-magnetic-resonance (NMR) study of ^{51}V in $V_3Ga_{1-x}Sn_x$ in both the normal and superconducting state. This system was chosen because of the large drop in T_c on going from V_3Ga to V_3Sn and because of the extensive band-structure calculations that have been made.[6,7] Since the vanadium atoms sit on linear chains in the $A15$ structure, the first band calculations were simple one-dimensional tight-binding calculations in nature. The dominant feature is very high narrow peaks in the density of states.[5] Later, Mattheiss[6] used the augmented-plane-wave (APW) method to calculate the band structure of a number of V_3X compounds. He showed there were large differences from the linear-chain model. He also noted that for X, a nontransition element, a rigid-band picture was fairly good. More recently, Goldberg and Weger[7] have used a tight-binding interpolation scheme to extend the high-symmetry-point calculations of Mattheiss to many more points in the Brillouin zone. They have calculated the four d-subband densities of states for V_3Ga and have argued that the APW

bands must be shifted to bring the large peak in the δ_2 subband density of states $N^{\delta_2}(E)$ to the Fermi energy.

The theory of spin-lattice relaxation in tetragonal symmetry using the tight-binding approximation appropriate for vanadium in the V_3X compounds is presented in Sec. II. Also presented in Sec. II is a description of the method of extracting the spectrum parameters: isotropic and axial Knight shifts, K_{iso} and K_{ax}, respectively, and the electric field gradient q. The experimental procedure is described in Sec. III. In Sec. IV, the experimental results are presented. In Sec. V, we discuss the NMR results and argue that they are consistent with the tight-binding interpolation based on the APW calculation of Mattheiss. A rigid-band model is appropriate for $V_3Ga_{1-x}Sn_x$, and a very high peak in the δ_2-subband density of states at E_F is inconsistent with the resonance results for V_3Ga. In Sec. VI, we conclude with some remarks about the temperature-dependent susceptibility for V_3Ga. We find that the large λ and therefore the high T_c for the Ga-rich compounds is correlated with large $N^{\pi}(0)$. This could result from a phonon softening due to anomalous electron dressing of the phonon states.

II. THEORY

A. Symmetry

The $A15$ (Cr_3O) structure in which the V_3X compounds crystallize is a cubic lattice with the X atoms on a bcc sublattice. We focus attention on the V sites that have tetragonal symmetry. The point group is $D_{2d}(\bar{4}2m)$ and the vanadium atoms lie on chains arranged in three orthogonal families. In Table I we list the irreducible representation of the d wave functions ($l=2$) for a vanadium atom on a chain with axis parallel to the $\bar{z}$ direction. Similar to the case of hcp metals, both Y_0^0 and Y_2^0 atomic wave functions belong to the A_1 representation of D_{2d}. Thus, the contact- and core-polarization interactions can interfer, provided these functions are admixed in the conduction-electron wave function at the Fermi surface.[8,9]

B. Spin-Lattice Relaxation

Following Narath,[8] we calculate the relaxation rate by treating the magnetic hyperfine interactions in terms of an effective-spin Hamiltonian,

$$\mathcal{H} = -\gamma_n \hbar \vec{I} \cdot \vec{h}, \tag{2.1}$$

where γ_n is the nuclear gyromagnetic ratio and $\vec{I}$ is the nuclear-spin angular-momentum operator. The effective-field operator $\vec{h}$ is composed of s contact ($\vec{h}_s$), d-spin core-polarization ($\vec{h}_d$), d-spin dipolar ($\vec{h}_{dip}$), and d-orbital ($\vec{h}_{orb}$) terms:

$$\vec{h} = \vec{h}_s + \vec{h}_d + \vec{h}_{dip} + \vec{h}_{orb}, \tag{2.2}$$

with

$$\vec{h}_s = -2H_{hfs}^{(s)} \vec{s}_s, \tag{2.3}$$

$$\vec{h}_d = 2H_{hfs}^{(d)} \vec{s}_d, \tag{2.4}$$

$$\vec{h}_{dip} = -\gamma_e \hbar r^{-3} [\vec{s}_d - 3\vec{r}^{-2}(\vec{r} \cdot \vec{s}_d)\vec{r}], \tag{2.5}$$

$$\vec{h}_{orb} = -\gamma_e \hbar r^{-3} \vec{l}, \tag{2.6}$$

where γ_e is the electronic gyromagnetic ratio, $\vec{s}_s$ and $\vec{s}_d$ are the s-spin and d-spin angular-momentum operators ($s=\frac{1}{2}$) for the conduction electrons, respectively; $\vec{l}$ is the orbital-angular-momentum operator for the d electrons ($l=2$), and $\vec{r}$ is the appropriate electron-position coordinate. We have assumed that the electronic g value may be taken as 2. The effect of the dipolar interaction on the relaxation rate is generally small and we neglect it. The effective s-contact and core-polarization (d-spin) hyperfine fields per electron are denoted by $H_{hfs}^{(s)}$ and $H_{hfs}^{(d)}$, respectively. The expectation value of r^{-3} in Eqs. (2.5) and (2.6) can be expressed in terms of an orbital hyperfine field per unit orbital angular momentum $H_{hfs}^{(orb)} = -\gamma_e \hbar \langle r^{-3} \rangle$. Straightforward application of first-order time-dependent perturbation theory to Eq. (2.1) yields a relaxation rate for a given site in the crystal

$$T_1^{-1} = (\pi/\hbar)(\gamma_n \hbar)^2 \sum_{\mu\mu'} \sum_{\vec{k}\vec{k}'} \sum_{\sigma\sigma'} |\langle \mu' \vec{k}' \sigma' | h^- | \mu \vec{k} \sigma \rangle|^2 \times f_{\mu\vec{k}\sigma}(1 - f_{\mu'\vec{k}'\sigma'}) \delta(\Delta E), \tag{2.7}$$

where μ, $\vec{k}$, and σ are the band, wave-vector, and spin indices, respectively, $f_{\mu\vec{k}\sigma}$ is the occupation number of the one-electron Block state $|\mu\vec{k}\sigma\rangle$, and the δ function $\delta(\Delta E)$ expresses the energy conservation requirements for the relaxation process. In the tight-binding approximation, the conduction-electron wave functions are constructed from atomic orbitals. For a lattice with an arbitrary basis, the result is

$$\psi_{\mu\vec{k}\sigma}(r) = N^{-1/2} \sum_j \sum_p e^{i\vec{k}\cdot\vec{R}_j} e^{i\vec{k}\cdot\vec{R}_p} a_{\mu\vec{k}}(\vec{r} - \vec{R}_{jp}) \phi_\sigma, \tag{2.8}$$

TABLE I. Irreducible representation of D_{2d} ($l=2$).

Bases	Assignment	Atomic functions	Spherical[a] harmonics
A_1	σ_z	$(5/4\pi)^{1/2} 3z^2 - r^2/2r^2$	Y_2^0
E	π_{1z}	$(15/4\pi)^{1/2} zx/r^2$	$Y_2^{1,c}$
E	π_{2z}	$(15/4\pi)^{1/2} zy/r^2$	$Y_2^{1,s}$
B_1	δ_{1z}	$(15/16\pi)^{1/2} x^2 - y^2/r^2$	$Y_2^{2,c}$
B_2	δ_{2z}	$(15/4\pi)^{1/2} xy/r^2$	$Y_2^{2,s}$

[a] $Y_l^{m,c} \equiv (Y_l^m + Y_l^{-m})/\sqrt{2}$; $Y_l^{m,s} = -i(Y_l^m - Y_l^{-m})/\sqrt{2}$; $Y_l^m(\theta, \phi)$ are normalized-spherical harmonics. The polar angle θ is measured with respect to a z axis parallel to the tetragonal or chain axis.

where N denotes the number of unit cells in the crystal, $\vec{R}_j$ specifies the location of a given unit cell, $\vec{R}_p$ specifies the atomic positions within the unit cell, and $\vec{R}_{jp}=\vec{R}_j+\vec{R}_p$. The ϕ_σ are spin functions, while the $a_{\mu\vec{k}}(\vec{r}-\vec{R}_{jp})$ are linear combinations of atomic orbitals (LCAO) defined by

$$a_{\mu\vec{k}}(\vec{r}-\vec{R}_{jp})=\sum_m c_{\mu m\vec{k}p}\,\phi_m(\vec{r}-\vec{R}_{jp}), \tag{2.9}$$

where the $c_{\mu m\vec{k}p}$ are elements of a unitary transformation and the $\phi_m(\vec{r}-\vec{R}_{jp})$ are atomic functions which form bases for irreducible representations of the point group appropriate for the position $\vec{R}_{jp}$. We also note that the functions [Eq. (2.8)] are not normalized unless all overlap-integrals between LCAO functions centered on different sites vanish.

The matrix elements in Eq. (2.7) can now be evaluated by expanding the Bloch functions according to the tight-binding prescription [Eq. (2.8)]. We assume that matrix elements between orbitals centered on different atoms can be neglected. This assumption is generally justified and is, moreover, consistent with the neglect of normalization in the tight-binding functions. We find the following relaxation rate for the pth site:

$$\begin{aligned}T_1(p)^{-1}=&(\pi/\hbar N^2)(\gamma_n\hbar)^2 k_B T\\ &\times\sum_{\mu\mu'}\sum_{\vec{k}\vec{k}'}\sum_{\sigma\sigma'}\delta(E_{\mu\vec{k}}-E_{\mu'\vec{k}})\,\delta(E_{\mu\vec{k}}-E_F)\\ &\times\sum_{mm'}F^{\Gamma(m)}_{\mu\vec{k}p}F^{\Gamma(m')}_{\mu'\vec{k}'p'}\left|\langle m'\sigma p\left|h^-\right|m\sigma p\rangle\right|^2,\end{aligned} \tag{2.10}$$

where k_B is Boltzmann's constant, E_F is the Fermi energy, and the $F^{\Gamma(m)}_{\mu\vec{k}p}\equiv|c_{\mu m\vec{k}p}|^2$ are fractional admixture coefficients which have the same value for all m forming a basis for a given irreducible representation $\Gamma(m)$. By defining average values of the $F^{\Gamma(m)}_{\mu\vec{k}p}$ according to

$$F^{\Gamma(m)}_p=\sum_\mu\sum_{\vec{k}}F^{\Gamma(m)}_{\mu\vec{k}p}[\delta(E_{\mu\vec{k}}-E_F)][N(0)N]^{-1}, \tag{2.11}$$

where the product $N(0)N$ is the total number of states per unit energy interval at the Fermi level for *one direction* of the spin, we can write Eq. (2.10) in the form

$$\begin{aligned}T_1(p)^{-1}=&(\pi/\hbar)(\gamma_n\hbar)^2 k_B T[N(0)]^2\\ &\times\sum_{mm'}\sum_{\sigma\sigma'}F^{\Gamma(m)}_p F^{\Gamma(m')}_p\left|\langle m'\sigma p\left|h^-\right|m\sigma p\rangle\right|^2.\end{aligned} \tag{2.12}$$

By definition, the factors $F^{\Gamma(m)}_p$ are normalized to unity:

$$\sum_m\sum_p F^{\Gamma(m)}_p=1. \tag{2.13}$$

Thus, we find

$$R=(4\pi/\hbar)(\gamma_n\hbar)^2 k_B[N(0)]^2\sum_i P_i^2(K_i^{(1)}+K_i^{(2)}\sin^2\theta), \tag{2.14}$$

where $R=(T_1T)^{-1}$,

$$\begin{aligned}&P_s=\rho H^{(s)}_{\rm hfs},\quad P_d=(1-\rho)H^{(d)}_{\rm hfs},\\ &P_{\rm orb}=(1-\rho)H^{(\rm orb)}_{\rm hfs}.\end{aligned} \tag{2.15}$$

ρ is the fractional s character at the Fermi level, θ is the angle between the tetragonal axis and the applied field, and

$$\begin{aligned}&K_s^{(1)}=1,\quad K_s^{(2)}=0,\\ &K_d^{(1)}=(F^{A_1})^2+\tfrac{1}{2}(F^E)^2+(F^{B_1})^2+(F^{B_2})^2,\\ &K_d^{(2)}=0,\quad K_{\rm orb}^{(1)}=2F^E(F^{B_2}+F^{B_1}+6F^{A_1}),\\ &K_{\rm orb}^{(2)}=-F^E(F^{B_2}+F^{B_1}+6F^{A_1}-\tfrac{1}{4}F^E).\end{aligned} \tag{2.16}$$

Summing over the three orthogonal vanadium chains in the cubic $A15$ structure, we find the θ-independent orbital reduction factor

$$K_{\rm orb}=\tfrac{4}{3}F^E(F^{B_2}+F^{B_1}+6F^{A_1}+\tfrac{1}{8}F^E), \tag{2.17}$$

with

$$F^{A_1}+2F^E+F^{B_1}+F^{B_2}=1.$$

If the A_1 functions are expressed as linear combinations of the form $\xi_{\mu\vec{k}}Y_0^0+(1-\xi_{\mu\vec{k}}^2)^{1/2}Y_2^0$, the s-d interference term is given by

$$\begin{aligned}R_{s-d}=&(8\pi/\hbar)(\gamma_n\hbar)^2[N(0)]^2 H^{(s)}_{\rm hfs}\quad H^{(d)}_{\rm hfs}\\ &\times\langle\langle(F_{\mu\vec{k}}{}^{A_1})^2\xi_{\mu\vec{k}}{}^2(1-\xi_{\mu\vec{k}}{}^2)\rangle\rangle,\end{aligned} \tag{2.18}$$

where the angular brackets denote an average over the Fermi surface. Since $H^{(s)}_{\rm hfs}$ and $H^{(d)}_{\rm hfs}$ are of opposite sign, this term interferes destructively with (2.14).

Although the relaxation rate for cubic-point symmetry is specified by a single d-electron orbital admixture parameter, and for hexagonal symmetry by two independent admixture parameters, the tetragonal-point symmetry requires three independent admixture parameters as a result of the lower symmetry.

The foregoing analysis contains two tacit assumptions. In the first place, it was assumed that the expansion of the conduction-electron wave functions at the Fermi level could be limited to $l=0$ and $l=2$ atomic functions [i.e., $N(0)=N_s(0)+N_d(0)$]. It is likely, however, that the $l=1$ admixture is often comparable to the $l=0$ admixture. Nevertheless, the $l=1$ hyperfine interaction may be safely neglected, since p hyperfine fields are generally quite small compared to s and d hyperfine fields. The major effect of an appreciable p admixture at the Fermi level is therefore to reduce $N(0)$ relative to the total bare-electron density of states by an amount which is proportional to the fractional p character. This reduction is probably small since the density of states is dominated in transition metals by the d-band contributions. A potentially more serious defect in the analysis is the assump-

tion that the four d orbitals have identical radial dependences. In other words, the d-spin and d-orbital hyperfine fields in Eqs. (2.4) and (2.6), respectively, are assumed to be constants. This assumption is reasonable only if the potential within the atomic volume is nearly spherically symmetric.

We have consciously ignored effects of electron-electron exchange enhancement on T_1, because the relaxation rate is dominated by the orbital hyperfine interaction (see Sec. V). The enhancement effect is spin coupled and would only enter the orbital relaxation rate via spin-orbit coupling, which is probably small in vanadium. In the absence of spin-orbit coupling, electron-electron enhancement would enter the relaxation rate through R_s and R_d as well as through R_{s-d}. As is well known, phonon renormalization effects do not enter the relaxation rate.

C. Nuclear Electric Quadrupole Interaction

In order to extract the electric field gradient (efg) q from the measured nuclear electric quadrupole interaction, a value of the nuclear quadrupole moment Q must be known. In our discussion we will use the value of $^{51}Q = 0.052$ b determined by Childs and Goodman.[10] Following the treatment of Watson, Gossard, and Yafet[11] (WGY), we write the measured efg as

$$q = (1-\gamma_\infty) q_{1\mathrm{att}} + (1-R_Q) q', \tag{2.19}$$

where $(1-\gamma_\infty)$ and $(1-R_Q)$ are the Sternheimer antishielding and shielding factors, respectively; $q_{1\mathrm{att}}$ is the point-charge contribution given by[11]

$$q_{1\mathrm{att}} = (1/a_0)^3 (15.6 Z_V - 5.9 Z_X), \tag{2.20}$$

where a_0 is the lattice parameter, Z_V and Z_X are the point charges of the vanadium and X sites, respectively, and q' is a local field gradient caused by the redistribution of occupied conduction-electron states near the Fermi surface. (We neglect q_0 and q'' of WGY that arise from nonspherical potential and orbital distortion, respectively.) The reader is referred to the paper by WGY[11] for detailed discussion of q'. Briefly, q' is the shielding response of the conduction electrons within the spherical potential of the APW sphere to the external potential imposed by the field gradient of point charges. It is therefore linear in $-q_{1\mathrm{att}}$ and related to the densities of states at the Fermi level for the various bands.

D. Analysis of Nuclear Electric Quadrupole and Anisotropic Shift Interaction on Powder-Pattern Line Shapes

In the following discussion we examine the effects of an axially-symmetric efg and an anisotropic Knight-shift interaction on the absorption pattern of a powder with random orientation of crystallite axes. We then describe a computer code for calculating synthetic absorption profiles by convoluting the powder patterns with a Gaussian line shape. Finally, we allow for a distribution of efg's and axial Knight shifts K_{ax}. The calculation is made to the second order in the nuclear electric quadrupole interaction for both the central $(+\frac{1}{2} \leftrightarrow -\frac{1}{2})$ transition as well as all satellite transitions.

Jones *et al.*[12] have shown that the nuclear Zeeman levels are obtained by adding together the expressions for the anisotropic shift (in first order) and for the nuclear quadrupole interaction (to second order). We shall suppose that the efg tensor and the magnetic shift tensor are both axially symmetric and that the major axes of the two tensors are parallel.

The zeroth order, or pure Zeeman, frequency is just the resonance frequency in the metal,

$$\nu_0 = \nu_R (1 + K_{\mathrm{iso}}). \tag{2.21}$$

Here ν_R is the resonance frequency in a diamagnetic reference compound and $K_{\mathrm{iso}} = \frac{1}{3} K_{\parallel} + \frac{2}{3} K_{\perp}$, where $K_{\parallel}$ and $K_{\perp}$ are the Knight shifts parallel and perpendicular to the major axis of the magnetic shift tensor, respectively.

The satellite frequencies are given in first order by[13]

$$\nu(m \rightarrow m-1) = \nu_0 \{1 + (3\mu^2 - 1)[a + \tfrac{1}{2}(\nu_Q/\nu_0)(m - \tfrac{1}{2})]\}, \quad m \neq \tfrac{1}{2}. \tag{2.22}$$

Here $\mu \equiv \cos\theta$ where θ is the angle between the external magnetic field H_0 and the Z axis of the principal axis system, $a \equiv K_{\mathrm{ax}}(\nu_R/\nu_0)$, where $K_{\mathrm{ax}} = \frac{1}{3}(K_{\parallel} - K_{\perp})$, and $\nu_Q = 3e^2 qQ/2I(2I-1)h$. For a random polycrystalline sample the principal maximum intensity for the satellites occurs when $\mu = 0$, so that resonance peaks appear at

$$\nu(m \rightarrow m-1) = \nu_0 \{1 - [a + \tfrac{1}{2}(\nu_Q/\nu_0)(m - \tfrac{1}{2})]\}, \quad m \neq \tfrac{1}{2}. \tag{2.23}$$

These peaks are shifted in second order by

$$\Delta\nu(m \rightarrow m-1) = -\tfrac{1}{16}(\nu_Q^2/\nu_0)[3m(m-1) - I(I+1) + \tfrac{3}{2}], \quad m \neq \tfrac{1}{2}. \tag{2.24}$$

The central transition in a single crystal is given to second order as

$$\nu(\tfrac{1}{2} \leftrightarrow -\tfrac{1}{2}) = \nu_0 \{1 + (\nu_Q^2/16\nu_0^2)[I(I+1) - \tfrac{3}{4}] \times (1-\mu^2)(1-9\mu^2) + a(3\mu^2 - 1)\}. \tag{2.25}$$

To compute a line shape appropriate to a polycrystalline sample, we have, following Cohen and Reif,[14] the shape function

$$P(\nu - \nu_0) d(\nu - \nu_0) = P(\theta) d\theta = \tfrac{1}{2} \sin\theta \, d\theta = \tfrac{1}{2} d\mu, \tag{2.26}$$

so that

$$P(\nu - \nu_0) = \tfrac{1}{2} |d\nu/d\mu|^{-1}, \quad -1 \leq \mu \geq 1. \tag{2.27}$$

The synthetic resonance is generated for each of several values of the efg and K_{ax} by folding the intensity distribution function $P(\nu - \nu_0)$ corresponding to Eq. (2.22) and (2.25) with the resonance shape function $g(\nu)$, which is taken as a Gaussian function with second moment $\langle \Delta\nu^2 \rangle$. Each resonance corresponding to a particular value of efg and

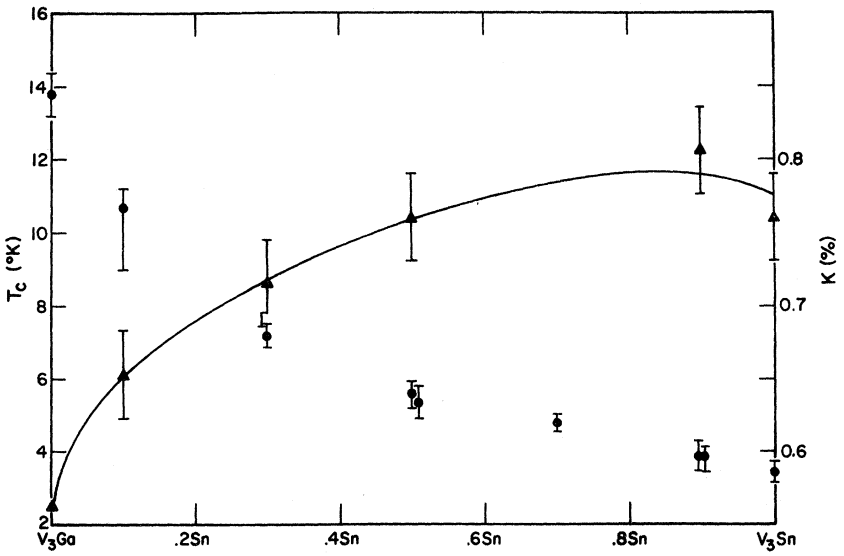

FIG. 1. Composition dependence of the superconducting transition temperature T_c (circles) and the 77 °K isotropic Knight shift K (triangles). T_c measurements were made on a Faraday balance; the bars indicate the width of the transition.

K_{ax} is then weighted according to the Gaussian function

$$G(q_i) = \exp\left(\frac{-2(q_i - q_0)^2}{(\Delta q)^2}\right) \Big/ \sum_i \exp\left(\frac{-2(q_i - q_0)^2}{(\Delta q)^2}\right), \tag{2.28}$$

where q_0 is the mean value of the efg distribution and $(\Delta q)^2$ is equal to four times the second moment of the efg distribution (K_{ax} is distributed in a similar manner). All of the resonance curves are placed upon a common frequency scale and summed. Typically, 11 to 25 values of q and K_{ax} are used in the final fits.

III. EXPERIMENTAL PROCEDURE

A series of pseudobinary compounds $V_3Ga_{1-x}Sn_x$ were prepared by arc melting (and levitation melting in the case of V_3Sn). The ingots were annealed at 1200 °C for 1 week followed by a 3-week anneal at 1000 °C and water quenching. Metallographic examination was made to determine the existence of second phases. In all cases, second phases accounted for less than 10–15% of the sample. Lattice parameters were determined from x-ray powder patterns. The superconducting transition temperature T_c was measured on a Faraday balance. The results are shown in Fig. 1. The vertical bars indicate the breadth of the transition. We note a rapid drop in T_c as Sn replaces Ga up to about $x = 0.3$ and then a much more gradual drop in T_c.

The NMR measurements were made on powders crushed from the ingots. Two phase-coherent pulsed spectrometers employing phase-sensitive detection were used. Measurements at 8 and 12 MHz were made on a fixed-frequency spectrometer with radio-frequency magnetic field amplitude H_1 between 100 and 150 Oe. The magnetic field was supplied by a Varian electromagnet with Fieldial control. Measurements near 18 and 48 MHz were made on a variable-frequency spectrometer with H_1 between 25 and 60 Oe. The magnetic field was supplied by a Westinghouse superconducting solenoid. Signal averaging was accomplished with both a Princeton Applied Research boxcar integrator and a Fabritek 952/1052 digital signal averager.

NMR measurements were made at room temperature, at 64 and 77 °K with the sample immersed in liquid nitrogen, and between 1.6 and 4.2 °K with the sample immersed in liquid helium. The ^{51}V nuclear-resonance profiles were obtained by integrating the echo following a two-pulse sequence. A boxcar gate much greater than the free-induction-decay time was used while the magnetic field was swept. T_1 measurements were made by saturating the nuclear-spin system with a comb of rf pulses and measuring the recovery of the longitudinal magnetization $M(\tau)$ at a time τ later. Single-exponential recovery was found in all cases, and nearly complete saturation was obtained (see Fig. 2).

The susceptibility of V_3Ga was measured in a temperature range from 16 up to 100 °K by the Faraday method. Although we found the susceptibility to be temperature dependent, it has a slightly weaker temperature dependence than that found by Clogston *et al.*[15] The weaker dependence may be due to the fact that our V_3Ga sample deviates from stoichiometry. Our V_3Ga has a somewhat lower value of T_c compared to the highest T_c reported for V_3Ga.[15]

IV. EXPERIMENTAL RESULTS

The NMR spectra of the ^{51}V nucleus was obtained for the $V_3Ga_{1-x}Sn_x$ system. The spectra were taken at 77 °K at three different frequencies, 8, 18, and 48.5 MHz. Figure 3 shows typical line shapes

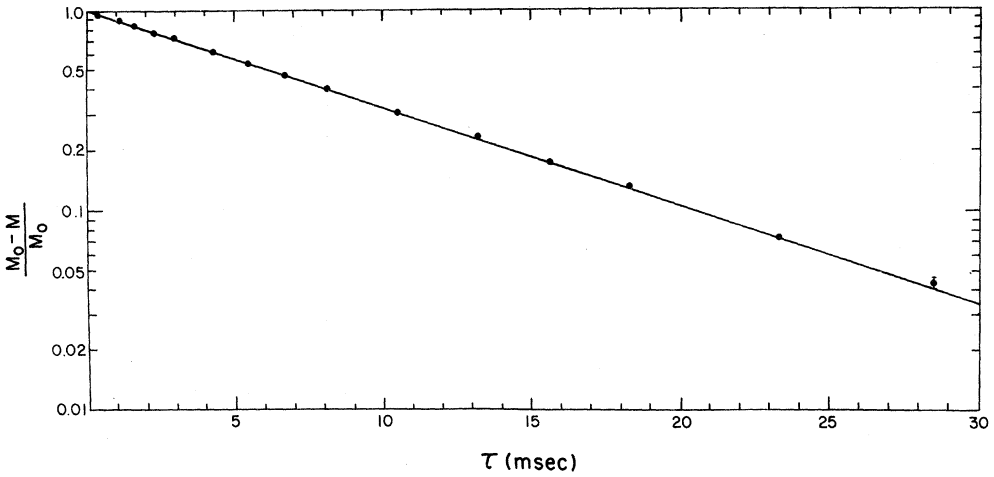

FIG. 2. Recovery curve of the longitudinal magnetization to its equilibrium value M_0 for $V_3Ga_{0.1}Sn_{0.9}$ at 77 °K.

of V_3Sn at 18 and 48.5 MHz. The difference in spectral shapes at these two frequencies is a result of the relatively large anisotropic Knight shift experienced by the ^{51}V nucleus. At 48.5 MHz the effect of this anisotropic Knight shift on the line shapes is about 2.7 times larger than at 18 MHz. Using the computer-generated line shapes, we find the anisotropic Knight shift K_{ax}, and the electric field gradient q seen by the ^{51}V nucleus for the $V_3Ga_{1-x}Sn_x$ system. The efg results are given in Fig. 4. K_{ax} is constant across the system and equal to -0.06%, while q is changing.

The peak of the line position was measured relative to Al metal. Using the computer-calculated line shift that results from the second-order quadrupole interaction and the anisotropic Knight shift, we get the isotropic Knight shift for the system. Figure 1 shows the isotropic-Knight-shift results at 77 °K.

T_1 of ^{51}V was measured in the $V_3Ga_{1-x}Sn_x$ system in the normal and in the superconducting states. In the normal state, T_1 shows the general temperature-dependent behavior previously found for the V_3X compounds, i.e., the higher-T_c compounds have stronger temperature dependencies.[16] Figure 5 shows the behavior for three different alloys. Figure 4 shows a plot of $1/T_1T$ for the $V_3Ga_{1-x}Sn_x$ system as a function of X at 77 °K. We see that there is moderate change in T_1 as a function of X at the Sn-rich side, while at the Ga-rich side there is a much faster change.

The temperature dependence of T_1 in the superconducting state was measured for all the alloys except V_3Ga. Two things characterize the behavior of T_1 in the superconducting state. First, there is a sharp decrease in the relaxation rate just below T_c compared to its value above T_c. Second, the relaxation rate depends exponentially on reciprocal temperature. Figure 6 shows a plot of T_1^{-1} as a function of $1/T$.

We were not able to obtain reliable T_1 data for V_3Ga in the superconducting state; heating effects due to long rf saturation pulse trains prevent us from getting data above 4.2 °K where the sample is not immersed in liquid He. Below 4.2 °K (far below T_c of V_3Ga), T_1 is long and there are spin-diffusion contributions to T_1.

V. DISCUSSION OF RESULTS

A. Normal State

In the discussion of our experimental values of q and $R = (T_1T)^{-1}$ we will rely on the band-structure calculations for V_3Ga by Mattheiss[6] and on the tight-binding interpolation scheme of Goldberg and Weger[7] based on these energy bands. Goldberg and Weger[7] have argued that the first-principle calculations of Mattheiss can be in error by as much as 0.2 Ry due to the choice of muffin-tin potential. In this section we will show that the d subbands calculated by Goldberg and Weger from the unadjusted bands of Mattheiss do, in fact, yield calculated values of the efg's and relaxation rates in excellent agreement with experiment.

In Fig. 7 we present the δ_2 and π d-subband densities of states calculated by Goldberg and Weger[7] from the original APW calculation of Mattheiss on V_3Ga. The theoretical δ_1 density is zero and the σ density is low and flat near E_F. Mattheiss's calculation is based on a $3d^4 4s^1$ vanadium configuration. A choice of $3d^3 4s^2$ yields results that are shifted by about 0.05 Ry. Mattheiss observed that when various nontransition elements X are used in the calculation of the V_3X band structure, the resulting densities of states nearly follow a rigid-band behavior. We will pursue this point of view and as-

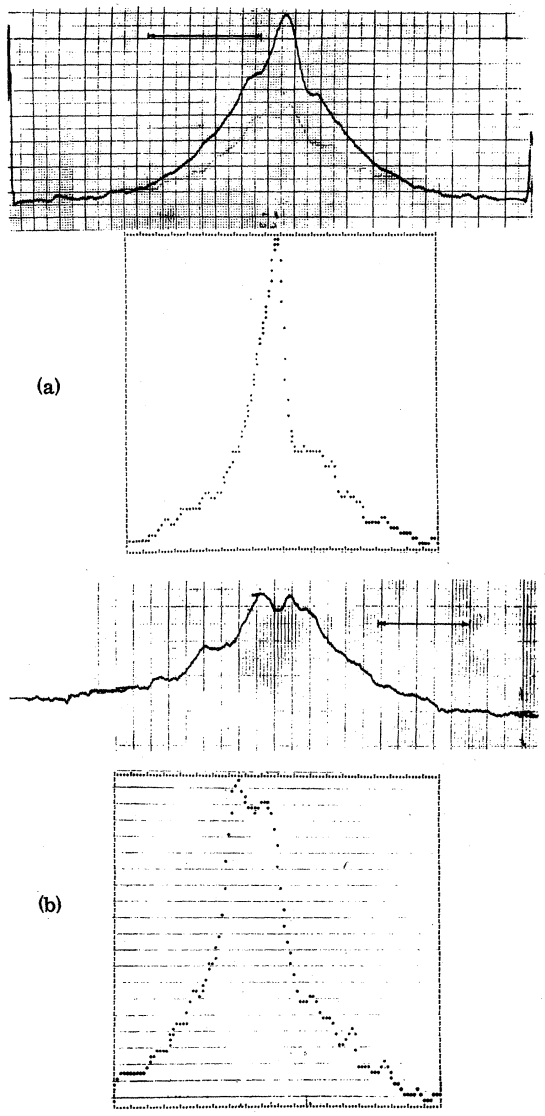

FIG. 3. Absorption spectra for V_3Sn obtained by integrating the echo following a two-pulse sequence as the field is swept at 77 °K. Top: experimental spectra (100 Oe scale). Bottom: computer-generated synthetic spectra (major division = 15.28 Oe). (a) $\nu = 18$ MHz. (b) $\nu \cong 48.5$ MHz. Magnetic field increases to the left.

sume that the replacement of Ga by Sn adds one additional conduction electron and merely shifts the Fermi energy E_F to higher values consistent with the total number of states required. This assumption places E_F for V_3Ga at 0.10 Ry and E_F for V_3Sn at 0.12 Ry (see Fig. 7).

Focusing attention on the terminal compositions V_3Ga and V_3Sn, we find that the use of the theoretical subband densities of states together with Eq. (2.14) yield values of R in fair agreement with the measured values, if we assume that the s fraction at the Fermi level ρ is near zero. The hyperfine fields are those used for vanadium metal by Yafet and Jaccarino[17]: $H_{hfs}^{(s)} = 1.12\times10^6$ Oe, $H_{hfs}^{(d)} = -0.117\times10^6$ Oe, $H_{hfs}^{(orb)} = 0.19\times10^6$ Oe. The contributions from spin-dipolar and -quadrupolar terms to the relaxation rate are negligible. In Table II, we compare the measured and calculated rates for V_3Ga and V_3Sn for $\rho = 0$ and $\rho = 0.1$. We see that even for $\rho = 0$ the calculated rates exceed the experimental rates by 12% for V_3Ga and 43% for V_3Sn.

If we now consider the measured values of q for V_3Ga and V_3Sn, we see [Eq. (2.19) and (2.20)] that in order to calculate q we must have values for the Sternheimer factors $1-\gamma_\infty$ and $1-R_Q$ as well as a reasonable point-charge assignment. We can set $1-R_Q$ equal to unity with no greater than 20% uncertainty. However, the other factors are difficult to calculate in a metal. We will turn the problem around. That is, for the theoretical d-subband densities, the dominant q' term is that involving the δ_2 and π subbands. This is referred to as case a of Fig. 4 of WGY.[11] Rearranging Eq. (2.19), we find

$$1-\gamma_\infty = q_{expt}/q_{1att} - q'/q_{1att} \,. \tag{5.1}$$

Using the values of $-q'/q_{1att}$ of Fig. 4 of WGY for the d-subband densities of Table II, yields a value of $(1-\gamma_\infty) \simeq 27$ for both V_3Ga and V_3Sn if we assign point charges of $Z_V \cong 1.8$, $Z_{Ga} \cong 3$, and $Z_{Sn} \simeq 4$ in Eq. (2.20). The values of Z are appropriate if the s and p conduction electrons are considered to be ionized and the d electrons localized on the atomic sites.

If we consider the distribution in efg's found at intermediate compositions to be dominated by the variation in Z_x from site to site we find

$$\frac{dq}{q} = \frac{dq_{1att}}{q_{1att}} = \frac{-5.9\,dZ_x/Z_x}{15.6\,Z_V/Z_x} \,, \tag{5.2}$$

which yields for $Z_V = 1.8$, $Z_x = 3.5$, and $dZ_x = 0.5$,

TABLE II. Spin-lattice relaxation in V_3Ga and V_3Sn.

	V_3Ga		V_3Sn	
$F^{\sigma 1}$	0.152		0.205	
F^{π}	0.273		0.333	
$F^{\delta 1}$	0.0		0.0	
$F^{\delta 2}$	0.303		0.128	
$N(0)$ states/Ry V	33		19.5	
ρ	0.1	0.0	0.1	0.0
R_{orb} [a]	2.62	3.40	1.32	1.63
R_d	0.351	0.433	0.09	0.113
R_s	2.61	0.0	0.91	0.0
R_{s-d}	−0.113	0.0	−0.07	0.0
R_{total}	5.47	3.83	2.25	1.75
R_{expt}	3.43		1.22	

[a] R in $[\text{sec}-(°\text{K})]^{-1}$.

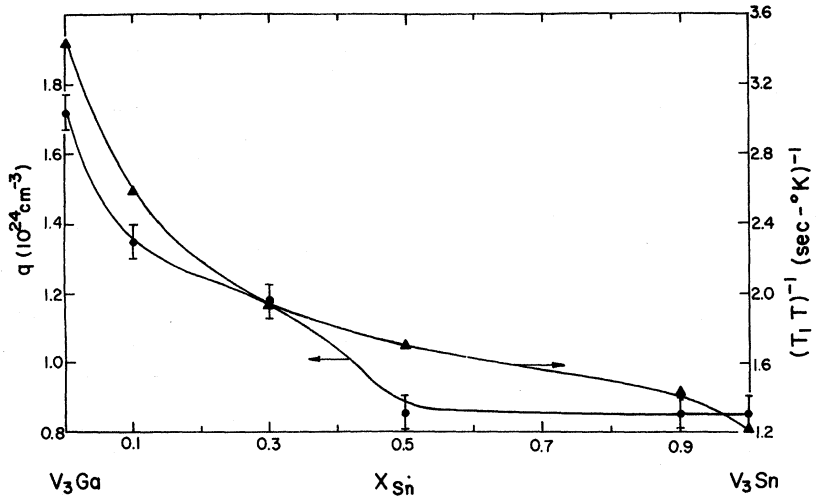

FIG. 4. Composition dependence of the electric field gradient q (circles) and the spin-lattice relaxation rate divided by the absolute temperature $(T_1T)^{-1}$ (triangles) at 77 °K.

a value of $dq/q = -0.40$. This is in reasonable agreement with the width of the distribution required in the synthetic spectra to fit the experimental line shapes. The point-charge assignments are somewhat arbitrary and suffer from lack of theoretical support. However, they have the virtue of self-consistent agreement with the mean efg's and the width of the distributions of efg's.

In Table III we list the calculated values of q_{latt} and q' assuming $(1-\gamma_\infty)=27$, $Z_V=1.8$, $Z_{Ga}=3$, and $Z_{Sn}=4$. Also listed in Table III is the value of $4F^{6}{}^{2}F^{\sigma}N(0)$ determined from case a of Fig. 4 of WGY for the calculated values of $-q'/q_{\text{latt}}$.

Because the theoretical $A_1(\sigma)$ subband density of states, between 0.10 and 0.12 Ry, is small and slowly varying,[7] we take $N^{\sigma}(0)$ to vary linearly from five states/Ry V at V_3Ga to four states/Ry V at V_3Sn. We now solve Eq. (2.14) with the additional assumptions that $\rho=0$ and $N^{\sigma 1}(0)=0$,[7] and using the values of $4F^{6}{}^{2}F^{\pi}(0)$ from Table III.

Table IV lists the calculated densities of states at E_F that brings the calculated relaxation rates in agreement with the experimental rates. We have used a value of $H_{\text{hfs}}^{(\text{orb})}=0.14\times10^{6}$ Oe. This value is 75% of the value used by Yafet and Jaccarino[17] for vanadium metal; their calculated relaxation rate exceeds the experimental rate. Use of $H_{\text{hfs}}^{(\text{orb})}=0.19\times10^{6}$ Oe yields an overestimate of R at $x=0.3$ and 0.5 by 20% and 50%, respectively. The use of a smaller value of $H_{\text{hfs}}^{(\text{orb})}$ results in a quantitative increase in $N^{\pi}(0)$ and $N(0)$ but no qualitative change in the shape of the densities of states. The d-subband densities and total densities of states are plotted in Fig. 8 and are in surprisingly good agreement with the shape and magnitude of the band-structure values (Fig. 7), assuming rigid-

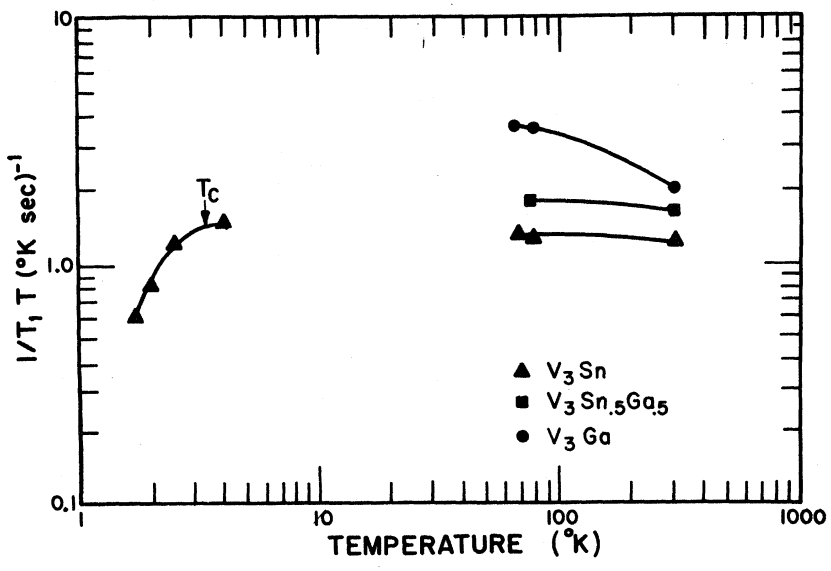

FIG. 5. Temperature dependence of the spin-lattice relaxation rate divided by the absolute temperature.

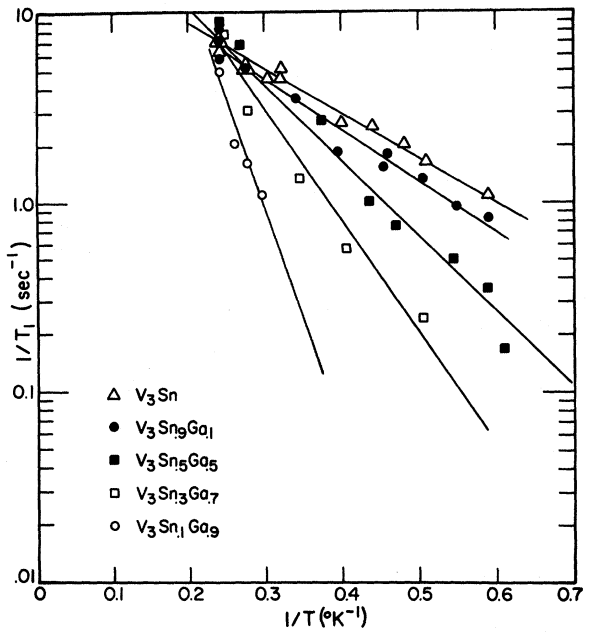

FIG. 6. Spin-lattice relaxation rate as a function of reciprocal temperature in the superconducting state.

band behavior, between 0.10 and 0.12 Ry.

In Table IV and Fig. 8, we have shown only one branch of the derived subband densities. The other solution would approximately reverse the roles of $N^{\pi}(0)$ and $N^{\delta 2}(0)$. This reversal, of course, would be in qualitative disagreement with the calculated subband densities of Fig. 7. Furthermore, in discussing the axial Knight shift we will show that the branch shown in Fig. 8 is the reasonable choice. We also note that the solution corresponding to high $N^{\delta 2}(0)$ on the tin-rich side yields values of $N(0) \gtrsim$ the renormalized density of states determined from the electronic specific heat, which is an unphysical result. The branch we choose as most reasonable corresponds to the orbital term dominating the relaxation rate. The other branch results in the d-spin core-polarization term dominating the relaxation rate.

The isotropic Knight shifts in the $V_3Ga_{1-x}Sn_x$ compounds are characterized by a rather constant value of the Van Vleck orbital term K_{iso}^{VV}. This is the part of the Knight shift that remains unchanged in the superconducting state since it does not depend on the unpaired-electron density at the Fermi level. The constancy of the value is further justification of the rigid-band approximation, since the Van Vleck term depends on all the conduction band states both below and above the Fermi level. In the normal state, we would expect the s-contact and the d-spin core-polarization term to yield positive and negative Knight shifts, respectively. In fact, for V_3Ga assuming the contact term is zero (consistent with $\rho = 0$ used to calculate the relaxation rates) leads to a core-polarization term of $K_{iso}^{d} = -0.14\%$ and a total isotropic Knight shift $K_{iso} = K_{iso}^{d} + K_{iso}^{s} + K_{iso}^{VV}$ of 0.50% compared to the experimental value of 0.56(2)%. The discrepancy could be removed by assuming incomplete quenching of the spin susceptibility in the superconducting state. removed by assuming incomplete quenching of the spin susceptibility in the superconducting state. V_3Ga also has a temperature-dependent Knight shift that results from the temperature dependence of the core-polarization term. This term is related to the d-spin susceptibility by $K_{iso}^{d} = H_{hfs}^{(d)} (\frac{1}{3}\chi^{(d)})/2\mu_B$.

The axial Knight shift K_{ax} is found to be roughly independent of concentration and equal to -0.06% in the $V_3Ga_{1-x}Sn_x$ compounds. The main contribution to the axial Knight shift comes from (a) the spin-dipolar interaction and (b) the anisotropy of the orbital susceptibility at the tetragonal sites.

To estimate the spin-dipolar contribution to K_{ax}, we follow the treatment of Boon.[18] His treatment leads to

TABLE III. Calculated q_{latt} and q' for $V_3Ga_{1-x}Sn_x$.

X	0.0	0.1	0.3	0.5	0.9	1.0
a_0(Å)	4.8155	4.8355	4.8730	4.9030	4.9610	4.9600
$a_0^3(10^{-24}$ cm$^3)$	111.7	113.1	115.7	117.9	122.1	122.0
q_{expt} [a]	1.72	1.35	1.18	0.86	0.86	0.86
q_{latt}	0.093	0.087	0.074	0.063	0.042	0.037
$(1-\gamma_\infty)q_{latt}$	2.511	2.349	1.998	1.701	1.134	0.999
q'	−0.791	−0.999	−0.818	−0.841	−0.274	−0.139
$-q'/q_{latt}$	+8.5	+11.5	11.1	13.3	6.5	3.8
$4F^{\delta 2}F^{\pi}N(0)$ states/Ry V	7	9	9	10	5	3

[a] q in 10^{24} cm^{-3}.

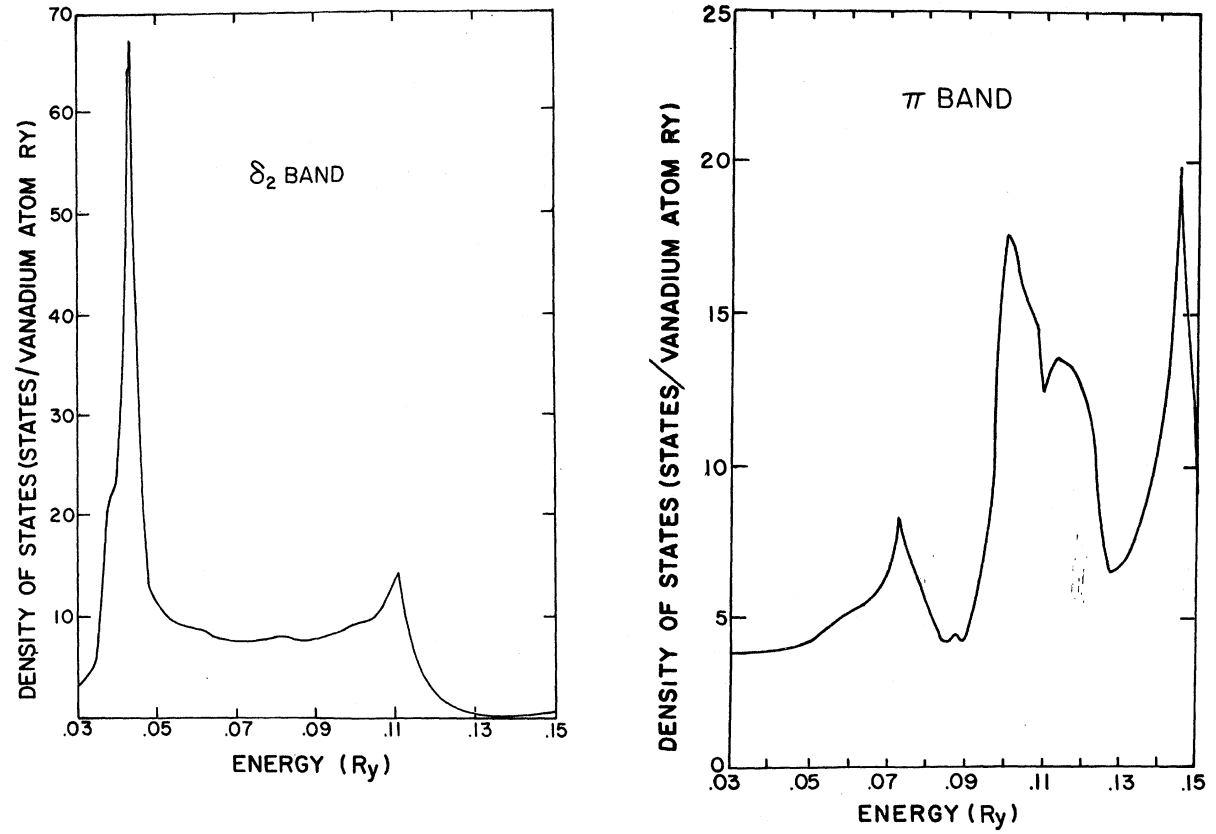

FIG. 7. The $\delta_2(B_2)$ and $\pi(E)$ subband densities of states in energy obtained from a tight-binding interpolation [Goldberg and Weger (Ref. 7)] of the APW calculations of Mattheiss (Ref. 6). (a) δ_2 subband. (b) π subband.

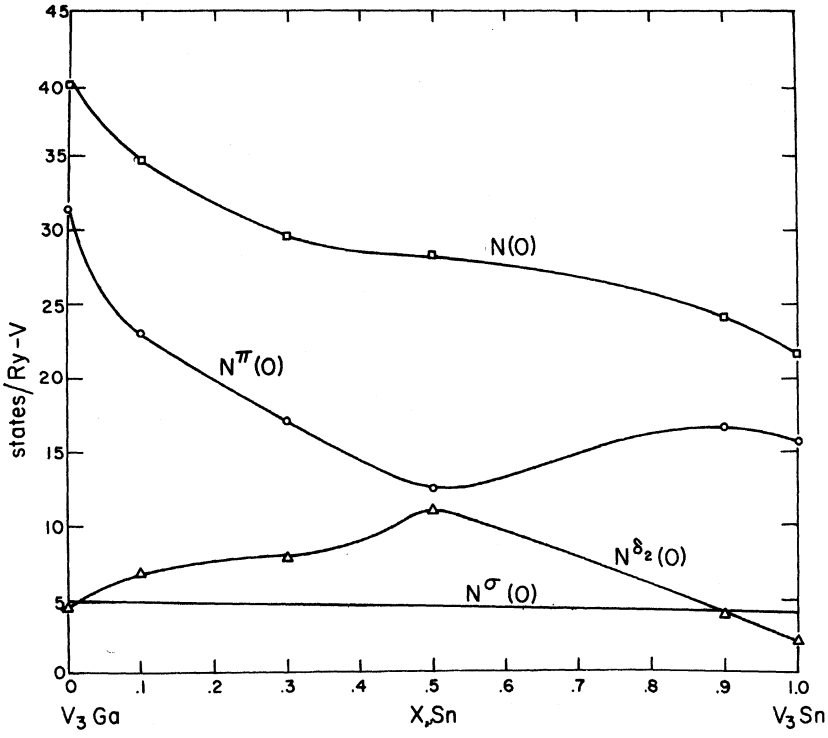

FIG. 8. Derived bare d-subband densities of states at the Fermi energy as a function of composition.

TABLE IV. Calculated densities of states, relaxation rates, and isotropic Knight shifts at 77 °K for $V_3Ga_{1-x}Sn_x$.

X	0.0	0.1	0.3	0.5	0.9	1.0
$4F^{\delta 2}F^{\pi}N(0)$ [a]	7	9	9	10	5	3
$N^{\sigma}(0)$	5.0	4.9	4.7	4.5	4.1	4.0
$N^{\pi}(0)$	31.5	23	17	12.5	16.6	15.5
$N^{\delta 2}(0)$	4.5	6.8	7.8	11	3.7	2.1
$N(0)$	41.0	34.7	29.5	28.3	24.4	21.6
R_{orb}	3.0	2.2	1.6	1.3	1.3	1.1
R_d	0.44	0.35	0.31	0.44	0.17	0.13
R_{total}	3.4	2.6	1.9	1.7	1.4	1.2
R_{expt}	3.43	2.59	1.94	1.71	1.43	1.22
K_{vv}(%) [b]	0.64	0.66	···	···	0.72	···
K_d(%)	−0.14	−0.12	−0.13	−0.13	−0.08	−0.07
$K_{vv}+K_d$(%)	0.50	0.54	···	···	0.64	···
K_{expt}(%)	0.56(2)	0.65(2)	0.71(2)	0.76(2)	0.80(2)	0.76(2)

[a]Densities of states in states/Ry V spin; R values in [sec-(°K)]$^{-1}$.
[b]Knight shift in the superconducting state assuming complete quenching of the spin susceptibility.

$$K_{ax}^{dip} = -\frac{1}{2}\int d^3\vec{r}'\,\frac{F'(\vec{r}')}{r'^3}\,P_2^0(\cos\theta'), \tag{5.3}$$

with

$$F'(\vec{r}') = g^2\mu_B^2 \sum_{\vec{k}} \frac{\delta f}{\delta E_{\vec{k}}} |\psi_k(\vec{r}')|^2. \tag{5.4}$$

Here $P_2^0(\cos\theta')$ is an associated Legendre polynomial, $\psi_{\vec{k}}(\vec{r}')$ are eigenfunctions of the electron Hamiltonian, g is the usual electron magnetic moment assumed equal to 2 for our case, μ_B is the Bohr magneton, and f is the Fermi function.

It is clear from the orthogonality of the Legendre polynomials that the angular part of $F'(\vec{r}')$ must transform as $P_2^{0'}$ for K_{ax}^{dip} to be nonvanishing. For purposes of our estimate, we will ignore the cross terms in $|\psi_{\vec{k}}(\vec{r}')|^2$ derived from a product of $l=1$ functions.

We consider instead the d-d terms. The result is

$$K_{ax}^{dip} = 2\mu_B^2\,\langle r^{-3}\rangle N(0)\,(2F^{\pi} - F^{\sigma} - \tfrac{1}{2}F^{\delta 1} - \tfrac{1}{2}F^{\delta 2}). \tag{5.5}$$

Note that for equal d-subband occupation, all the $F^{(i)}$'s = 0.2 and $K_{ax}^{dip} = 0$. Approximating $2\mu_B\langle r^{-3}\rangle$ by $H_{hfs}^{(orb)} = 0.14\times10^6$ Oe, we find that $K_{ax}^{dip} = +0.15\%$ for V_3Ga and $+0.06\%$ for V_3Sn. Thus, we require a negative value of K_{ax}^{VV} to fit the experimental values. If instead of using the subband densities of Fig. 8, we use the large $F^{\delta 2}$ solution for V_3Ga, we would get a value of $K_{ax}^{dip} = -0.10\%$ for V_3Ga. This would require a change of sign of K_{ax}^{VV} between V_3Ga and V_3Sn to explain the constancy of the experimental value of K_{ax}. We believe this is unlikely since K_{ax}^{VV} depends on states well removed from E_F.

B. Superconducting State

Our T_1 data in the superconducting state show the typical behavior found for T well below T_c, namely, $1/T_1 = A\exp[-\Delta(0)/k_BT]$, where $2\Delta(0)$ is the superconducting energy gap at $T=0$. Figure 6 is a plot of $1/T_1$ vs $1/T$. From the slopes of these lines we determine the energy gap of the alloys.

The Bardeen-Cooper-Schrieffer (BCS)[19] theory gives a simple relation between T_c and the energy gap:

$$2\Delta(0) = 3.5\,k_BT_c. \tag{5.6}$$

In Table V we list the values of T_c, $2\Delta(0)$, and the ratio $2\Delta(0)/k_BT_c$ for the different alloys. We see that $2\Delta(0)/k_BT_c$ is below the BCS value for $X=0.9$ and 1.0, equal to the BCS value for $X=0.5$, and greater than the BCS value for $X=0.1$ and 0.3. The low values of $2\Delta(0)/k_BT_c$ for $X=0.9$ and 1.0 is probably due to the fact that the experimental temperature is not sufficiently below T_c to use the simple exponential asymptotic form for T_1.

Geilikman and Kresin[20] have recently shown that the relation between the energy gap and transition temperature in a strong-coupled superconductor

TABLE V. Superconducting transition temperature and energy gap in $V_3Ga_{1-x}Sn_x$.

X	0.0	0.1	0.3	0.5	0.7	0.9	1.0
T_c(°K)	13.8	10.7	7.2	5.6	4.8	3.8	3.4
$2\Delta(0)$ (meV)	···	4.4(6)	2.3(2)	1.8(1)	···	1.03(5)	0.84(5)
$2\Delta(0)/k_BT_c$	···	4.7(7)	3.7(3)	3.6(2)	···	3.2(2)	2.9(2)

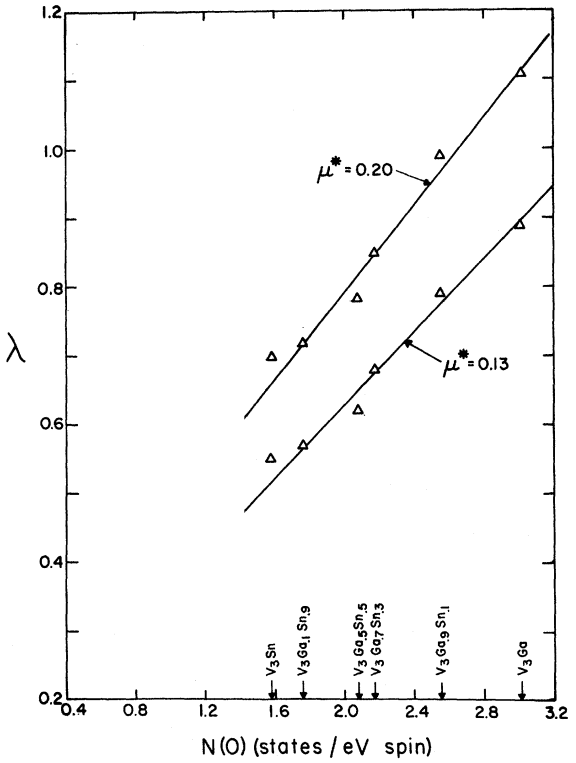

FIG. 9. Electron-phonon coupling parameter λ as a function of the bare density of states at the Fermi level.

is given by

$$2\Delta(0) = 3.52\,T_c[1 + 5.3\,(T_c^2/\omega_0^2)\ln(\omega_0/T_c)],$$

where ω_0 is the frequency of the lower of the two model-phonon peaks and not equal to the Debye frequency. It seems that in the $V_3Ga_{1-x}Sn_x$ system a phonon softening (decreasing ω_0) occurs close to the Ga-rich side.

VI. CONCLUSIONS

It appears from the agreement of our results with the calculated densities of states that the large peak at 0.04 Ry in the δ_2 subband (see Fig. 7) does not fall at the Fermi level in V_3Ga. Although the sharp peak was derived from the linear-chain model[5] and the high value of $N(0)$ was necessary to explain early electronic specific-heat data[7] (extrapolated from above T_c), our relaxation data does not allow for such a large peak in the density of states at E_F. The relaxation result is a strong limitation on $N(0)$ since relaxation rates are additive. In fact, the peak in $N(0)$ found for V_3Ga is probably due to the π subband.

Based on the peak in the $\pi(E)$ subband at V_3Ga we find a value of $T_F = (170 \pm 40)$ °K, $T_F^2 = \frac{1}{2}[-d^2 \ln[N^\pi(E)]/dE^2]_{E=E_F}$. This can be compared to the low-temperature susceptibility using the equation, valid for small Coulomb enhancement

$$\chi = \chi_0[1 - \tfrac{1}{12}\pi^2(T/T_F)^2]. \qquad (6.1)$$

Our low-temperature susceptibility results on V_3Ga yield a value of T_F of about 210 °K.

If we calculate the electron-phonon coupling parameter λ:

$$\lambda = \frac{N(0)\langle I^2\rangle}{M\langle\omega\rangle/\langle\omega^{-1}\rangle}, \qquad (6.2)$$

where $\langle I^2\rangle$ is the average over the Fermi surface of the electron-ion matrix element, M is the ion mass, and $\langle\omega^m\rangle$ are appropriate phonon averages, with the McMillan[2] equation

$$T_c = \frac{\theta_D}{1.45}\exp\left(-\frac{1.04(1+\lambda)}{\lambda - \mu^*(1+0.6\lambda)}\right), \qquad (6.3)$$

we find the values of λ plotted in Fig. 9. Here we have taken $\mu^* = 0.13$ and 0.20 and $\Theta_D = 310$ °K. The dependence of λ on $N(0)$ for constant μ^* is approximately given by $\lambda = 0.16 + 0.31\,N(0)$ for $\mu^* = 0.20$ and $\lambda = 0.09 + 0.27\,N(0)$ for $\mu^* = 0.13$. Of course, the use of a constant μ^* is probably incorrect, as is the use of the McMillan equation for the $A15$ compounds, which have anomalous phonon spectra.

We may compare our derived value of $N(0)$ with that determined from specific-heat measurements. Spitzli[21] has found the electronic specific-heat term of V_3Sn to yield a phonon-renormalized value of 1.85 states/eV V spin. Compared to our $N(0)$ value this yields a $\lambda = 0.17$. For V_3Ga, Junod *et al.*[15] find the enhanced value of 7.035 states/eV V spin. Thus we find $\lambda = 1.33$ for V_3Ga. However, recent specific-heat measurements by Knapp and Jones[22] on a sample of V_3Ga with a T_c of 14.5 °K and NMR parameters essentially unchanged from those reported in this paper yield a renormalized density of states of 5.65 states/eV V spin. Compared to our derived bare-density of states this yields a value of $\lambda = 0.87$, which is in good agreement with their value of $\lambda = 0.64 \pm 0.3$ derived from extrapolation to $T = 0$ °K of the high-temperature bare-density of states.

It has been argued[1,2] that for fairly high $N(0)$ metals the numerator in Eq. (6.2) is approximately independent of $N(0)$. In fact, Allen and Cohen[23] have shown that for two similar materials A and B, where A has a high T_c and anomalous softening of the phonon spectrum, and B a low T_c and normal-phonon spectrum, the difference in electron-phonon coupling parameter $\Delta\lambda \equiv \lambda_A - \lambda_B$ can be written

$$\Delta\lambda = (C/N)\sum_{\vec{q}}[\omega_{\vec{q}}^2(B)/\omega_{\vec{q}}^2(A) - 1], \qquad (6.4)$$

where C is a constant of order $\frac{1}{2}$ and N is the number of phonon modes. Although in Fig. 9 we find an approximately linear dependence of λ on $N(0)$, the difference $\lambda(V_3Ga) - \lambda(V_3Sn)$ can be understood in terms of phonon softening, i.e., a decrease in

$\omega_{\vec{q}}^2(V_3Ga)$ in Eq. (6.4). We note the correlation of high λ with large $N^{\pi}(0)$. From Table I, we see that the π subband corresponds to d-wave functions whose lobes point in the [011] and [101] directions, where we are focusing on a vanadium atom on a Z-axis chain. This spatial direction corresponds to the direction of atomic motion for a phonon propagating in a $[01\bar{1}]$ direction with transverse polarization along [011]. This is the so-called soft phonon found in $A15$ structures. A high π-subband density corresponds to a greater localization of the d electrons of this symmetry, i.e., effectively smaller atoms in the [011] directions and thus softer phonons. In other words, the bare-phonon frequencies are renormalized by electron dressing effects which tend to diminish the phonon frequencies as the π-subband density of states increases towards V_3Ga.

ACKNOWLEDGMENT

The authors would like to thank Dr. G. S. Knapp for the T_c measurements and for helpful discussions. Dr. M. Weger kindly provided details of his subband densities of states and made useful comments on the manuscript. J. W. Downey, B. C. Huguelet, and R. A. Conner provided experimental assistance. G. T. Bowdin performed continuous-wave NMR measurements on three of the samples, allowing us a check on our spectrum fitting procedure.

---

*Work performed under the auspices of the U.S. Atomic Energy Commission.

†Permanent address: Soreq Nuclear Research Center, Yavne, Israel.

[1]K. H. Bennemann and J. W. Garland, AIP Conf. Proc. **4**, 103 (1972).

[2]W. L. McMillan, Phys. Rev. **167**, 331 (1968).

[3]G. Gladstone, M. A. Jensen, and J. R. Schrieffer, in *Superconductivity II*, edited by R. D. Parks (Marcel Dekker, New York, 1969).

[4]F. Y. Fradin and P. D. Neumann, in *Treatise on Materials Science II*, edited by H. Herman (Academic, New York, 1973), Chap. X; A. C. Gossard, Phys. Rev. **149**, 246 (1966); L. R. Testardi and T. B. Bateman, Phys. Rev. **154**, 402 (1967).

[5]A. M. Clogsten and V. Jaccarino, Phys. Rev. **121**, 1357 (1961); F. I. Morin and J. P. Maita, Phys. Rev. **129**, 1115 (1963); J. Labbe, S. Barisic, and J. Friedel, Phys. Rev. Lett. **19**, 1039 (1967).

[6]L. F. Mattheiss, Phys. Rev. **138** A112 (1965).

[7]I. B. Goldberg and M. Weger, J. Phys. C **4**, L188 (1971); M. Weger and I. B. Goldberg, in *Solid State Physics*, edited by F. Seitz, D. Turnbull, and H. Ehrenreich (Academic, New York, 1973); extensive references to the literature on the V_3X compounds can be found in this excellent review.

[8]A. Narath, Phys. Rev. **162**, 320 (1967). More complete discussions of the contact, orbital, and core polarization contributions to nuclear spin-lattice relaxation can be found in J. Korringa, Physica (Utr.) **16**, 601 (1950); Y. Obata, J. Phys. Soc. Jap. **18**, 1020 (1963); and Y. Yafet and V. Jaccarino, Phys. Rev. **133**, A160 (1964), respectively.

[9]J. W. Ross, F. Y. Fradin, L. L. Isaacs, and D. J. Lam, Phys. Rev. **183**, 645 (1969).

[10]W. J. Childs and L. S. Goodman, Phys. Rev. **156**, 64 (1967); W. J. Childs, Phys. Rev. **156**, 71 (1967).

[11]R. E. Watson, A. C. Gossard, and Y. Yafet, Phys. Rev. **140**, A375 (1965).

[12]W. H. Jones, Jr., T. P. Graham, and R. G. Barnes, Phys. Rev. **132**, 1898 (1964).

[13]B. R. McCart and R. G. Barnes, J. Chem. Phys. **48**, 127 (1968).

[14]M. H. Cohen and F. Reif, in *Solid State Physics*, edited by F. Seitz and D. Turnbull (Academic, New York, 1957).

[15]A. M. Clogston, A. C. Gossard, V. Jaccarino, and Y. Yafet, Phys. Rev. Lett. **9**, 262 (1962); W. E. Blumberg, J. Eisinger, V. Jaccarino, and B. T. Matthaiss [Phys. Rev. Lett. **5**, 149 (1960)] report a value of $T_c \simeq 16.5$ °K for stoichiometric V_3Ga. However, recent heat capacity work [A. Junod, J. L. Staudenmann, J. Muller, and P. Spitzli, J. Low Temp. Phys. **5**, 25 (1971)] yields a value of T_c between 14.9 and 15.1 °K for stoichiometric V_3Ga. A study of the effect of stoichiometry in V_3Ga on the NMR of ^{51}V will be published separately [F. Y. Fradin and G. S. Knapp (unpublished)].

[16]B. G. Silbernagel, M. Weger, W. G. Clark, and J. H. Wernick, Phys. Rev. **153**, 535 (1967).

[17]Y. Yafet and V. Jaccarino, Phys. Rev. **133**, A1630 (1964).

[18]M. H. Boon, Physica (Utr.) **30**, 1326 (1964).

[19]J. Bardeen, L. N. Cooper, and J. R. Schrieffer, Phys. Rev. **108**, 1175 (1957).

[20]B. T. Geilikman and V. Z. Kresin, Phys. Lett. **40A**, 123 (1972).

[21]P. Spitzli, Phys. Kondens. Mater. **13**, 22 (1971).

[22]G. S. Knapp and R. W. Jones, Bull. Am. Phys. Soc. **18**, 327 (1973).

[23]P. B. Allen and M. L. Cohen, Thirteenth International Conference on Low Temperature Physics, Boulder, Colo. (unpublished).